Hygrothermal and Acoustical Performance of Starch-Beet Pulp Composites

Hamzé Karaky, Chadi Maalouf, Christophe C. Bliard, Tala Moussa, Nadim El Wakil, Mohammed Lachi, Guillaume Polidori

Hygrothermal and acoustical performance of various Starch-Beet pulp composites

Hamzé KARAKY[1,2*], Chadi MAALOUF[1], Christophe BLIARD[2], Tala MOUSSA[1], Nadim EL WAKIL[1], Mohamed LACHI[1], Guillaume POLIDORI[1].

[1] Groupe de Recherche en Sciences de l'Ingénieur GRESPI, SFR Condorcet FR CNRS 3417, Université de Reims Champagne Ardennes, Moulin de la Housse, BP 1039, 51687 Cedex 2, France.

[2] Institut de Chimie Moléculaire de Reims, ICMR-UMR 7312 CNRS, Université de Reims Champagne Ardennes, Moulin de la Housse, BP 1039, 51687 Cedex 2, France.

*Corresponding author; e-mail: hamze.karaky@etudiant.univ-reims.fr

Abstract

This article deals with the elaboration and the characterization of an innovative bio-concrete 100 % plant-based made solely on Beet pulp (BP) and potato starch (S). Using this type of material in insulation applications seems a good solution to reduce the CO_2 gas emissions in building. The influence of the starch amount was studied. Four mixtures are considered with different mass ratio S/BP (0.1, 0.2, 0.3 and 0.4). Physical properties of these materials were studied in terms of porosity, apparent and absolute density, thermal conductivity, and hygric properties. The influence of humidity content on acoustical properties was studied a function of frequency. Results show a real impact of both starch and humidity contents on hygrothermal and acoustical properties of the studied material due to the porosity. The composite with the lowest amount of starch (S/BP=0.1) seems to be the optimal composition in terms of hygrothermal and acoustical behavior.

Keywords

Bio-based composite, starch-Beet pulp, porosity, thermal conductivity, sorption isotherm, moisture buffering value, permeability, acoustical performance.

Introduction

The building sector is responsible for approximately 50% of total energy consumption and 11% of CO_2 gas emissions. Therefore, it has become crucial to turn to renewable energy and resources as well as ecofriendly and sustainable materials especially in building applications in order to

reduce both environmental impacts and primary energy use. The use of bio-based composites recently in construction appears to be a promoting solution while maintaining high indoor comfort [1–6].

Several studies have been already published on the use of crop by-products for buildings. Hemp concrete is the most studied among different composite materials [7–11]. Hemp-starch composite presents a porous structure providing a good thermal insulation with a thermal conductivity ranges from 0.06 W. m-1. K-1 to 0.1 W. m^{-1}. K^{-1}. It is also classified as an excellent humidity regulator. The moisture buffering value (MBV) measured between 2.6 g. m^{-2}. % RH^{-1} and 2.7 g. m^{-2}. % RH^{-1}. The impact of both size particles and starch content was also studied [7]. The water vapor permeability of the hemp-lime concrete obtained by Collet et al is high (1.7 x 10^{-10} kg m^{-1} s^{-1} Pa^{-1}).

The porosity of several bio-based composites was reported in [2,7,12] as well as the influence of both porosity and water content on the composites properties. The results show that the hygrothermal properties increase with porosity of the composite. In another study, hygric properties such as sorption isotherm, water vapor permeability, and moisture buffer capacity MBV of a bio-based materials such as hemp concrete, flax concrete and rape straw concrete, were presented [13]. The results showed that these materials have a low thermal conductivity but a high MBV, which provides a good hygrothermal insulating capacity.

Many studies have investigated the acoustical performance of hemp-starch composites [10,14–16]. The hemp-starch composite is a good acoustical insulator due to its porous structure. Hemp-starch composite can absorb 70 % of the sound waves for medium and high frequencies. The sound absorption coefficient is independent of the composite porosity. In this paper, authors deal with the study of starch-Beet pulp composite for building applications.

Sugar beet (*Beta Vulgaris*) is widely grown in France (8 million tons/year) and used in sugar factory to produce the white sugar. Sugar beet pulp is a byproduct and mainly used to produce the feed for livestock due to the high nutritional value [17,18]. It is mechanically compressed using an extrusion machine to obtain the extruded beet pulp (BP). In this article, BP was used to elaborate the beet pulp-starch composite. The beet pulp is an important source of pectin which has been evaluated in many studies [19–21]. BP is used in food, cosmetics industries, as well as a bio-adsorbent for the removal of heavy metals [22]. Cement-beet pulp concrete was studied by Monreal et al [23] where an important dimensional deformation is observed. Many physico-

chemical treatments were carried out for the beet pulp to reduce its hydrophilic nature. The linseed oil treatment was the optimal treatment which reduce the aggregates ability to absorb water and swell.

Starch is a kind of sugar and contains two polymers with different primary structure, Amylose (linear chain) where glucose units are joined by α 1-4 glycosidic bonds and Amylopectin (branched chain) where the glucose chains are branched onto α 1-6 positions [24]. Starch is a hydrophilic material and exists in many plants such as cereals (30 % to 70 %), tubers (60% to 90 %) and legumes (25 % to 50 %) [25–27]. It is used in paper factory, textile and food factories via the beverage, confectionery and baked goods industries [28,29]. It can be also used to produce bio-ethanol and pharmaceutical products by fermentation process [30]. The present work aims to elaborate a bio-sourced material made of BP and potato starch designed to be used in the building sector for walls and roof insulation applications. The hygrothermal and acoustical characteristics of this material are determined and fitted analytically.

1. Materials and Methods

1.1.Extruded beet pulp

The 8-10 mm diameter extruded beet pulp pellets BP (18% humidity) (see Figure 1 a, b and c) were provided by Cristal Union factory (Pomacle, France). To ensure proper conservation in the lab the pulps were kept at -20°C until use. Before use, extruded beet pulp (BP) was immersed in water for two hours and dried at 50 °C (see Figure 1d). The dominate size of extruded beet pulp dried is comprise between 2 mm and 4 mm (see Figure 2). It can be noted that the BP dried presents a rough surface which provides a good adhesion with starch binder. BP is lightweight and porous material (see Table 1). BP contains mainly pectin, hemicellulose and cellulose (see Figure 3).

Table 1: porosity and densities of BP.

Aggregates	ρ_{app} (kg. m^{-3})	ρ_{abs} (kg. m^{-3})	Porosity (%)
Fresh beet pulp	134 ± 6.7	911.61 ± 45.6	85.30
Extruded beet pulp	194 ± 7.9	1073.38 ± 53.7	81.93

Figure 1: (a) Sugar beet fruit, (b) fresh sugar beet pulp, (c) extruded beet pulp pellets and (d) extruded beet pulp dried.

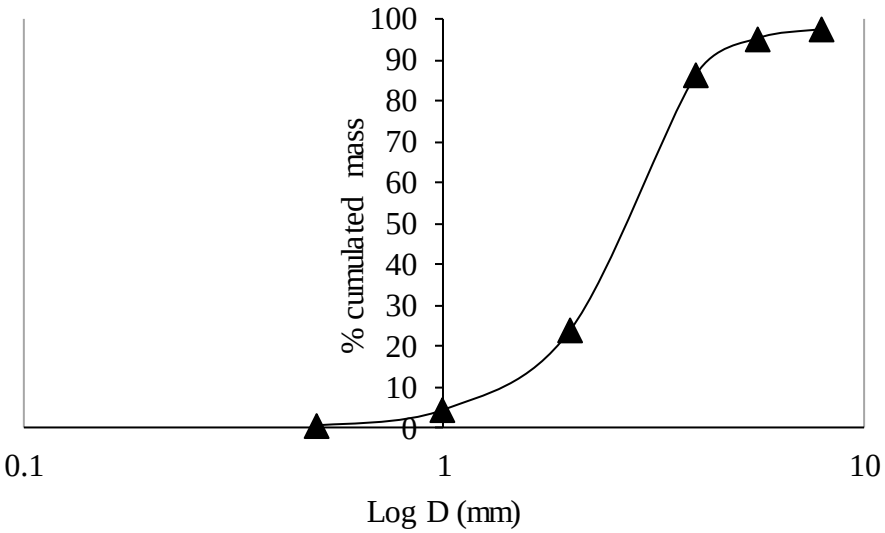

Figure 2: Grain size distribution curve of BP.

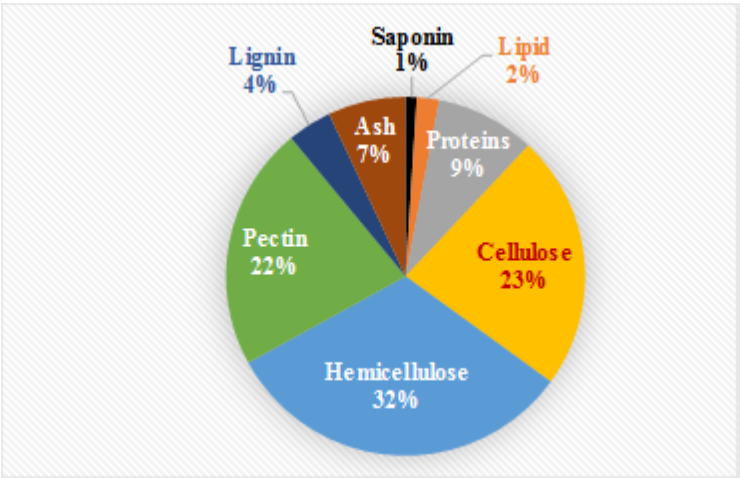

Figure 3: The components of the BP [31].

1.2.Potato starch

Potato starch was purchased from ROQUETTE, Lestrem, France. Potato starch has a high polymerization degree which gives a viscous binder and provides a good mechanical property for the BP – starch formulas (see Figure 4 a). Starch was used as binder to make a several bio-composite such as hemp-starch and palm date fibers-starch [7,9,10,32]. It can stick the particles together and ensure the transmission of shear forces between the fibers. The starch grains can penetrate in the BP pores thanks to its small size which provides a good adhesion between the components (see figure 4 b).

(a)

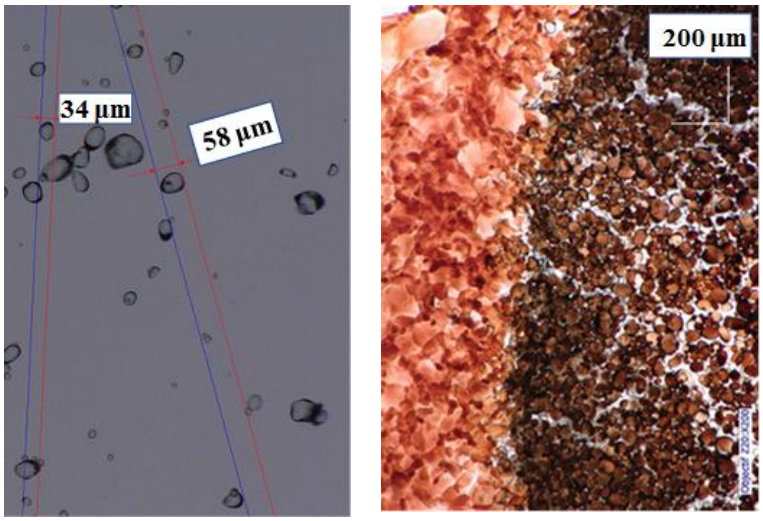

(b)

Figure 4: (a) Powder of potato starch (b) Potato starch grains.

1.3.Composite formulations

Starch and sugar beet pulps are hydrophilic materials, due to their great ability to store water molecules in their structure. This imposes a competition between these two components to absorb

water from the mixture resulting a binder with undissolved starch grains and a mixture of wet pulps. Several studies have proposed to prepare the binder separately, with an optimum dynamic viscosity and surface tension [10,16]. In our case, this solution was not effective enough, due to the hydrophilic behavior of the pulps which causes a significant water gradient all around the sample during drying, and consequently causes dimensional deformations. For this reason, a new preparation method is used which does not require any water addition. To avoid water competition between beet pulps and starch grains, extruded pulps were soaked in distilled water to ensure saturation with a mass ratio Water / BP = 2.5 [23]. The wet BP is then mixed with starch powder. The mix was putted in an autoclave to dissolve the starch under water vapor pressure. After that, samples were compacted using the traction machine INSTRON 8801 at 44 kPa. Finally, the mix was frozen and dried using a freeze dryer, then put in a climatic chamber at 50 °C and 10 % RH to achieve the drying procedure.

Four formulations with four different S/BP mass ratios (0.1, 0.2, 0.3 and 0.4) were prepared to study the starch amount influence on the composite behavior (see Figure 5).

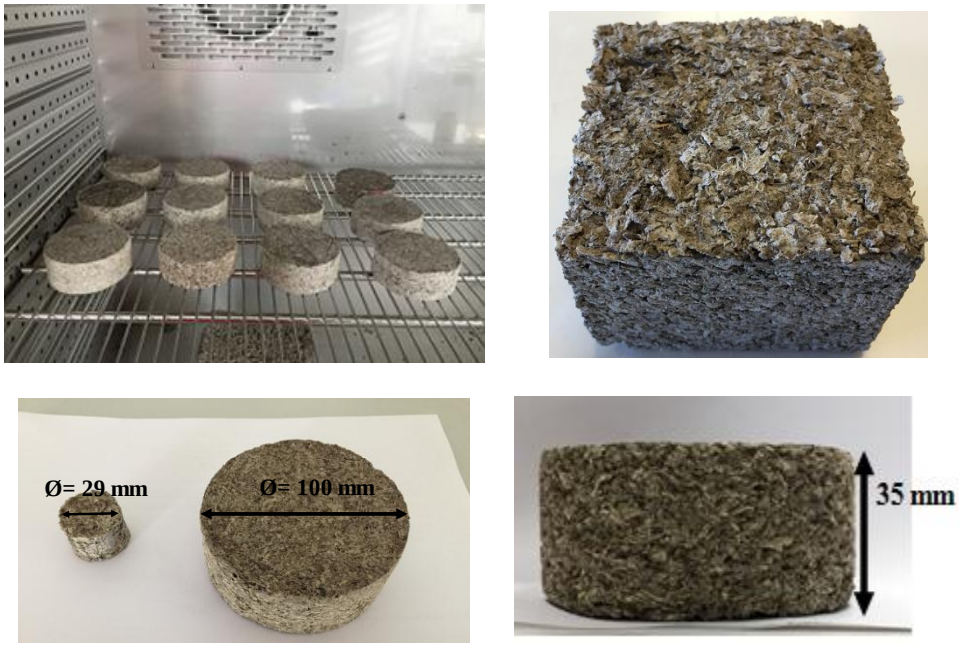

Figure 5: Composites specimens obtained from the four formulations.

1.4.Density and porosity

The absolute density of starch-beet pulp composite was calculated using the pycnometer method [2,7]. The pycnometer was filled with a given mass of dried pulp and half its volume with cyclohexane, which is a non-polar solvent and does not affect the composition and mass of the pulp (M). The system undergoes 6 cycles of boiling (30 minutes) and cooling (10 minutes), during these cycles, air escapes from the pulp leaving its pores, and cyclohexane replaces it, and during the 6th cycle, the system is kept under an argon atmosphere to avoid humidity. At room temperature (20 ° C), the pycnometer was filled to the end and plugged with the stopper. The system was then weighed with an accuracy of 10^{-3} g. The absolute density is calculated according to the equation (1):

$$\rho_{abs} = \frac{M_1 \times \rho_{cyc}}{M_1 - (M_2 - M_3)} \quad (1)$$

with ρ_{abs} is the absolute density (kg. m^{-3}), ρ_{cyc} is the density of cyclohexane (kg. m^{-3}), M_1 is the dry aggregates mass, M_2 is mass of the pycnometer filled with cyclohexane and saturated aggregates) and M_3 is the pycnometer mass (cyclohexane).

Precautions have been taken to avoid the residual moisture accumulation in the reflux system. Each measurement was performed at least 3 times to be considered representative.

The porosity and pore structure of the composite was measured using mercury intrusion porosimetry (MIP) [9,33]. The pore access radius is from 1 μm to 1000 μm.

1.5.Sound absorption coefficient

The Kundt tube type BK 4206 (tube with two fixed microphones) was used in this section to measure the sound absorption coefficient α. This device consists of a cylindrical tube with two ¼ inch BK type 4187 microphones, a BK 2706 power amplifier and an OROS analyzer. For the sound absorption measurements, two tubes of varied sizes were used to change the frequency ranges (see Figure 6).

(a) (b)

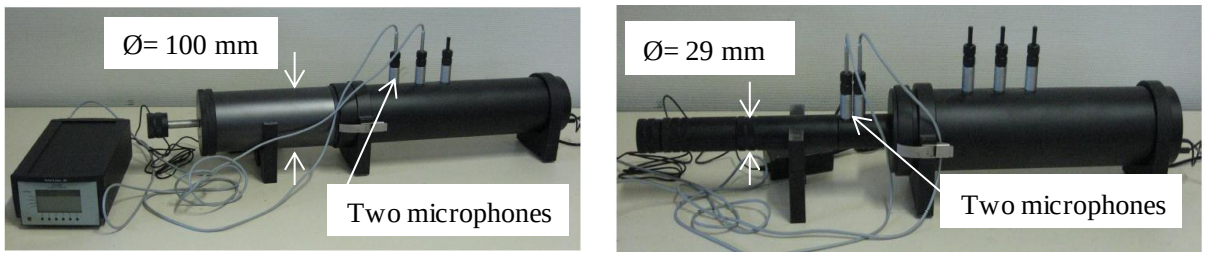

Figure 6: (a) Kundt tube used to measure the sound absorption coefficient for (a) low frequencies and (b) high frequencies.

The Kundt tube is able to measure the acoustic absorption as well as the surface impedance according to the NF EN ISO 10534-2 standard. The used device for this test contains two microphones spaced a variable distance depending on the tube, a loudspeaker attached to an extremity of the tube, and the sample placed on the other extremity. By using the analyzer generator and power amplifier, the speaker is excited with white noise. Both microphones detect reflected and incident sound pressures. The principle of measurement of sound absorption is therefore based on the study of the transfer function H between two signals picked up by these two microphones.

1.6. Thermal conductivity

The thermal conductivity of BP-S composite was measured using ISOMET 2114 Applied Precision [34]. The heat flow is generated by heating an electrical resistor inserted into the sample hole to assuring a direct heat contact with the sample. Thermal conductivity evaluation is based on the temperature measurements taken periodically as a function of time. The tested cubic samples (see Figure 5) tested were dried using a climatic chamber at 50 °C and 10 %RH. Before the measure, the samples dried were cooled and stabilized at 23 °C and 10 % RH. Samples are covered during the test to avoid the humidity absorption (see Figure 7).

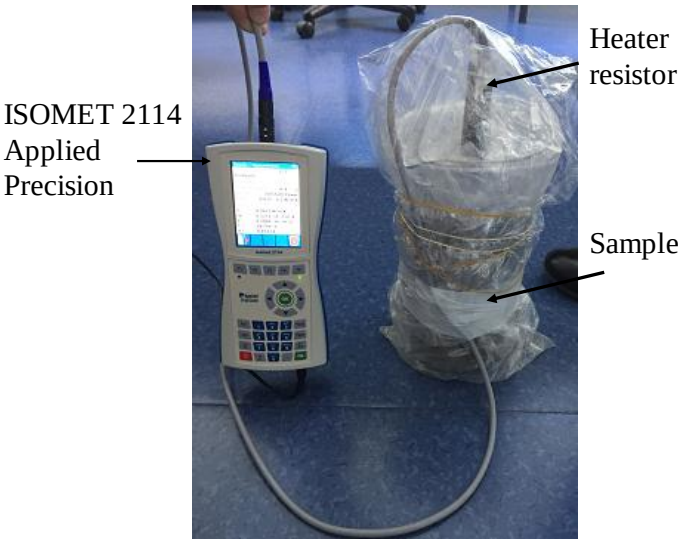

Figure 7: ISOMET 2114 Applied Precision for the thermal conductivity measurements.

Regarding the theoretical thermal conductivity for the agro-materials solid phase, it was evaluated at 20 °C using the representation of Collet et al [35] and Rahim et al [13] shown in Figure 8. The effective thermal conductivity was given as a function of both thermal conductivities of the solid phase air in the equation (2) where n is the total porosity, λ_a the air thermal conductivity, λ_s the solid phase thermal conductivity, and λ_{eff} the experimental thermal conductivity.

$$\lambda_{eff} = \lambda_s \times (1 + \frac{n}{(\frac{1-n}{3}) + \frac{1}{(\lambda_a/\lambda_s - 1)}}) \quad (2)$$

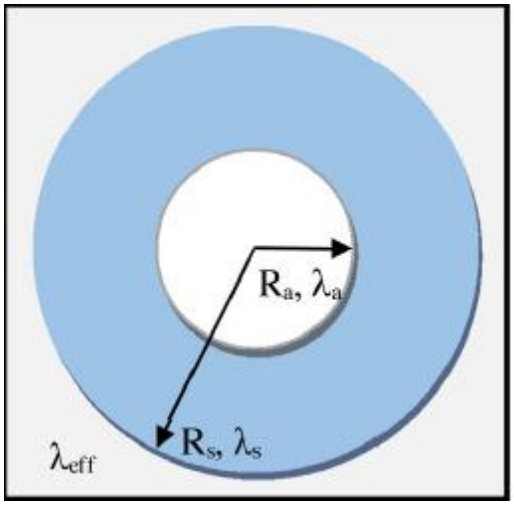

Figure 8: Agro-material geometry considered as a two-phase medium in a homogeneous equivalent medium [7].

The heat capacity of the S/BP composite was measured using a C80 Calvet calorimeter from Setaram Instrumentation. In the calorimetric detector, the sample and the cell reference were completely surrounded by an array of thermocouple detectors allowing the heat transfer measurement including radiation, convection, and conduction.

1.7.Permeability

Water vapor permeability δ_v (kg. m^{-1}. s^{-1}. Pa^{-1}) represents the capacity of water vapor to pass through the material under steam flow pressure. The measurement was carried out according to the NF EN ISO 12571, using the dry cup method [2,10]. The samples were dried in a climatic chamber at 50 °C and 10 % RH (see Figure 9 a). The sample is sealed at the top of the cup which contains the silica gel at its bottom, providing a 0% RH (see Figure 9 b). The overall was placed in a climatic chamber set to 50 % RH at 23 °C. The water vapor resistance factor μ and δ_v are given in equations (3) and (4). Where *G* the mass rate (kg. s^{-1}), ΔP_v the vapor pressure gradient, *e* the thickness of the sample, *A* the exposed surface area (m^2), and δ_a the air water vapor permeability.

$$\delta_v = \frac{G \times e}{\Delta P_v \times A} \quad (3)$$

$$\mu = \frac{\delta_a}{\delta_v} \quad (4)$$

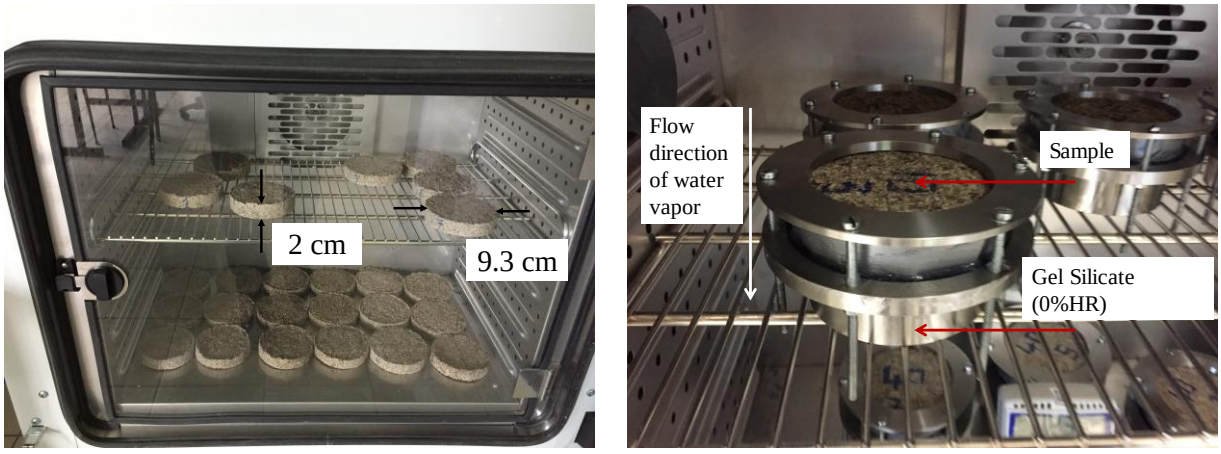

(a) (b)

Figure 9: (a) samples in climatic chamber at 50 °C and 10 % RH (b) Dry cup method for vapor permeability measurements.

1.8.Sorption isotherm

The sorption isotherm tests are carried out in accordance with NF EN ISO standard 12572 (2001) [2,9]. They allow to plot the sorption curve representing the variation of the water content variation as a function of relative humidity of ambient air at a constant temperature of 23 °C. The sorption isotherm shows, in other terms, the equilibrium between water content in the composite and relative humidity [36].

Four cylindrical samples of 10 cm diameter and 4 cm thickness per mixture were prepared (see figure 5). They were dried for 7 days at 50°C and 10% RH until they reach the dry state. Then they were placed in a climatic chamber at 23°C and at various RH levels: 20 %, 40 %, 60 %, 80 %, and 92 %. At each humidity level, measurements were carried out until mass variation for three successive weighs is less than 0.1% of the total mass. Experimental results were then fitted with three analytical models: GAB [37] , Merakeb [38], and Van Genuchten [39].

Experimental data were correlated with the least squares method. To estimate the variability attributed to each model, the correlation coefficient (R^2) is calculated. The mean deviation E and root mean square error (RMSE) were also evaluated. These criteria allow to judge the quality of the adjustment of experimental results with respect to the model. They are defined in equation (5) and (6).

$$E = \frac{100}{N} \times \Sigma_{i=1}^{n} \frac{|m_e^i - m_p^i|}{m_e^i} \quad (5)$$

$$RMSE = \sqrt{\frac{\Sigma_{i=1}^{n} (m_e^i - m_p^i)^2}{N}} \quad (6)$$

where m_e the experimental measure, m_p the value computed using the model and N the total number of experimental values. The adjustment between experimental and analytical values is considered correct when the mean relative deviation does not exceed 10%. The adjustment quality is inversely proportional to E and RMSE values.

1.9.MBV

The Moisture Buffering Value represents the capacity of the composite to regulate the relative humidity of a medium. The Nordtest protocol defines cyclic step-changes in relative humidity after stabilization, between high (75%) and low (33%) values for 8 and 16 h, respectively [7–9,11,40].

Four 10 cm diameter and 4 cm thick cylindrical samples were tested for each formula. The edges and back-sides of samples were sealed with duct tape to obtain a one-dimensional moisture flow. Samples were stabilized at 23° C and 50% RH in a climatic chamber and weighed until they reached equilibrium. During the periodic exposure, samples were weighed five times during the adsorption phase and twice during desorption. When the mass variation between three consecutive days is under 5%, the experiment was stopped and the moisture buffering value (MBV) was calculated according to the equation (7):

$$MBV = \frac{\Delta m}{A \times (RH_{high} - RH_{low})} \quad (7)$$

A (m^2) is the sample area that is in contact with air. The RH_{high} and RH_{low} respectively represent high relative humidity (75 % RH) and low relative humidity (33 % RH), and Δm represents the mass change during the absorption / desorption phase (g).

2. Results and discussions

2.1. Porosity analysis

Figure 10 shows the apparent density variation of the fully dried composite material in the climatic chamber at 50 ° C and 10% RH, as a function of S / BP mass ratio. It can be observed that the density increases linearly with mass ratio S / BP. Apparent density varies from 271.4 $kg.m^{-3}$ to 360 $kg.m^{-3}$. It should be noted that the average apparent density of Beet Cement-Pulp concrete is between 570 $kg.m^{-3}$ and 770 kg. m^{-3} [23] . The apparent density of the samples can be expressed as a function of mass ratio S / BP between 0.1 and 0.4 by equation (8).

$$\rho = 295.42 \times \left(\frac{S}{BP}\right) + 242.8 \quad (8)$$

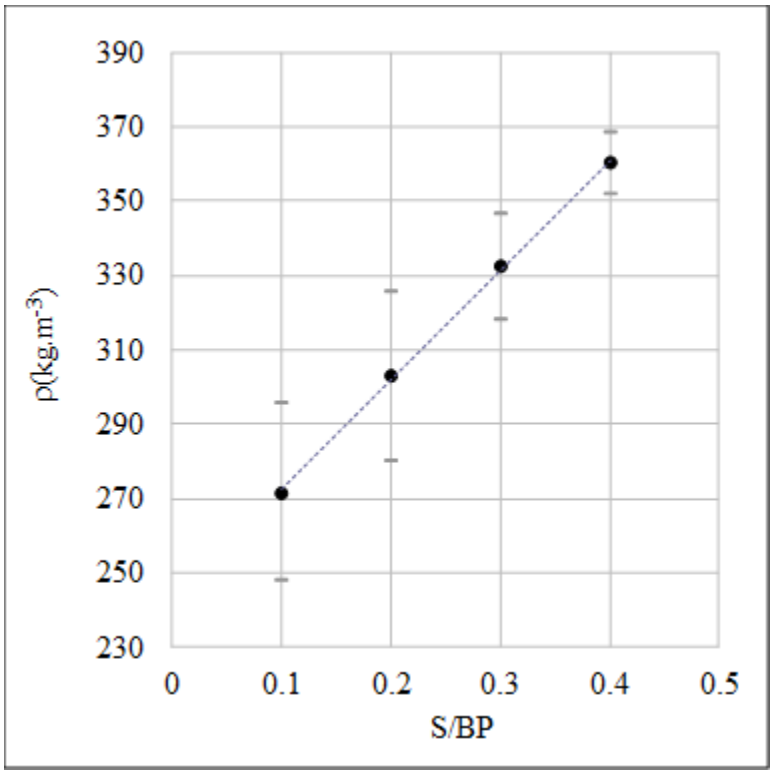

Figure 10: Apparent density evolution with S/BP mass ratio.

Density and porosity results are shown in Figure 11. Absolute and apparent density increase with the S/BP ratio. However, the porosity of the composite decreases logarithmically. Therefore, the sample with the lowest amount of starch (S / PB = 0.1) has the highest porosity (79.75%) and the lowest absolute density (ρabs = 1222 kg.m^{-3}). The total porosity was between 70.60% and 79.75% and the decrease in the S / BP ratio appears to increase the total porosity. The influence of starch in a agreement with the results obtained by Rahim et al. [13] and Bourdot et al [7]. The presence of starch gel increases the apparent density and decreases the total porosity by filling the inter-particle space between the pulp particles sealing the pores. Therefore, the composite would contain closed and open pores more or less accessible.

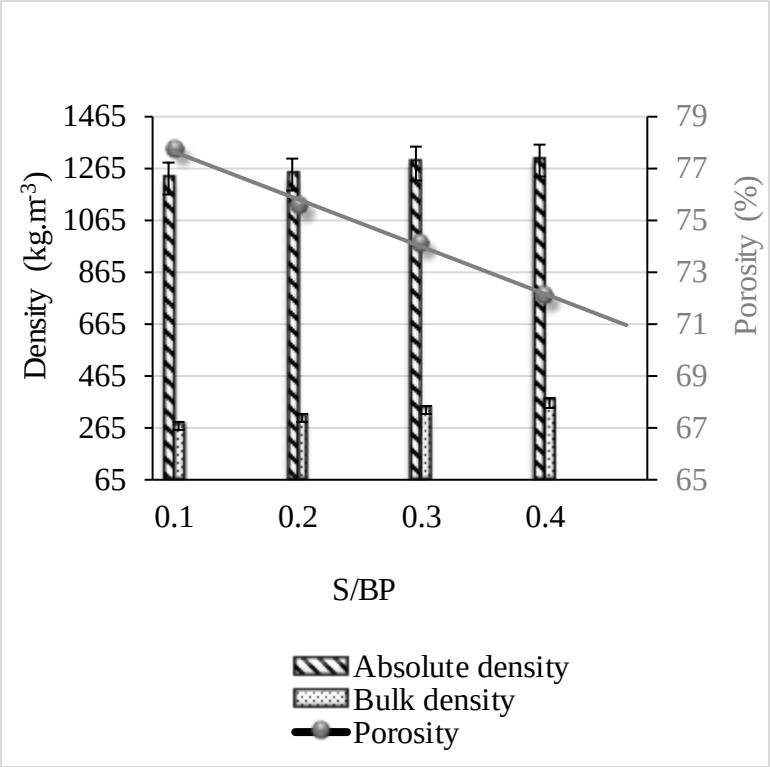

Figure 11: the density and the porosity of BP composite measured by cyclohexane method.

Bourdot et al studied the density and porosity of hemp particles of two different sizes 0-5 mm and 0-20 mm, the results show that small particles have a density and a porosity smaller than that of large particles, respectively 1266 $kg.m^{-3}$ and 89.3% and 1271 $kg.m^{-3}$ and 91.3% [7]. The absolute density and the porosity of the hemp-starch agro-materials were similar whatever the composition, with approximately 1240 $kg.m^{-3}$ and 89%. However, the absolute density increases slightly with the hemp/starch ratio (H/S) and the proportion of 0-20 mm hemp [4,10]. The presence of potato starch gel increases apparent density and decreases total porosity by filling the inter-specific pores between aggregates. This can be explained by the creation of closed pores between the aggregates and the gel. It can thus be noted that the agro-materials are composed of a closed porosity and open more or less accessible. The MIP method (Mercury Intrusion porosimetry) was used to see the accessible porosity which influences the agro-material properties, in particular the hygroscopic properties.

Mercury porosimetry allowed us to study the influence of the mass ratio S/BP. The four curves show a similar cumulative pore volume. The mercury first filled the small pores to fill the large pores. From Figure 12 , we notice two classes of access radius are identified: macro pores (> 150

μm), meso-pores (1-150 μm). Figure 12 shows the analysis of the measurement of porosity under mercury pressure. It should be noted that the accessible porosity of the starch-BP material is bonded to the binder due to the porous nature of the starch gel as deduced from the results obtained with the pycnometer method. The sample with a mass ratio S/BP = 0.1 is the most porous with a total porosity 66%. The porosity of the composite decreases with the increase of the mass ratio S/BP to reach a value around 60%. The total porosity depends on the binder content (potato starch). The pore distribution of each composition shows that the volume of the macro-pores decreases with the increase of the binder content, and that the volume of the meso-pores increases in the formula (S/PB = 0.4). The existence of the meso-pores is entirely due to the morphology of the aggregate and the starch content. Mesopores were created in the composite by increasing the S/BP mass ratio to 30%, which appears to be a critical ratio at which the starch continues to plug the voids in the composite. The porosity measured by the pycnometer method decreases linearly from 77.79 % to 72.16 % when the weight ratio S/BP increases from 0.1 to 0.4. The absolute density increases by 1222.18 $kg.m^{-3}$ 1293.42 $kg.m^{-3}$. The absolute mass of potato starch which is around 1451.19 $kg.m^{-3}$ explains the increase in the absolute mass of the composite.

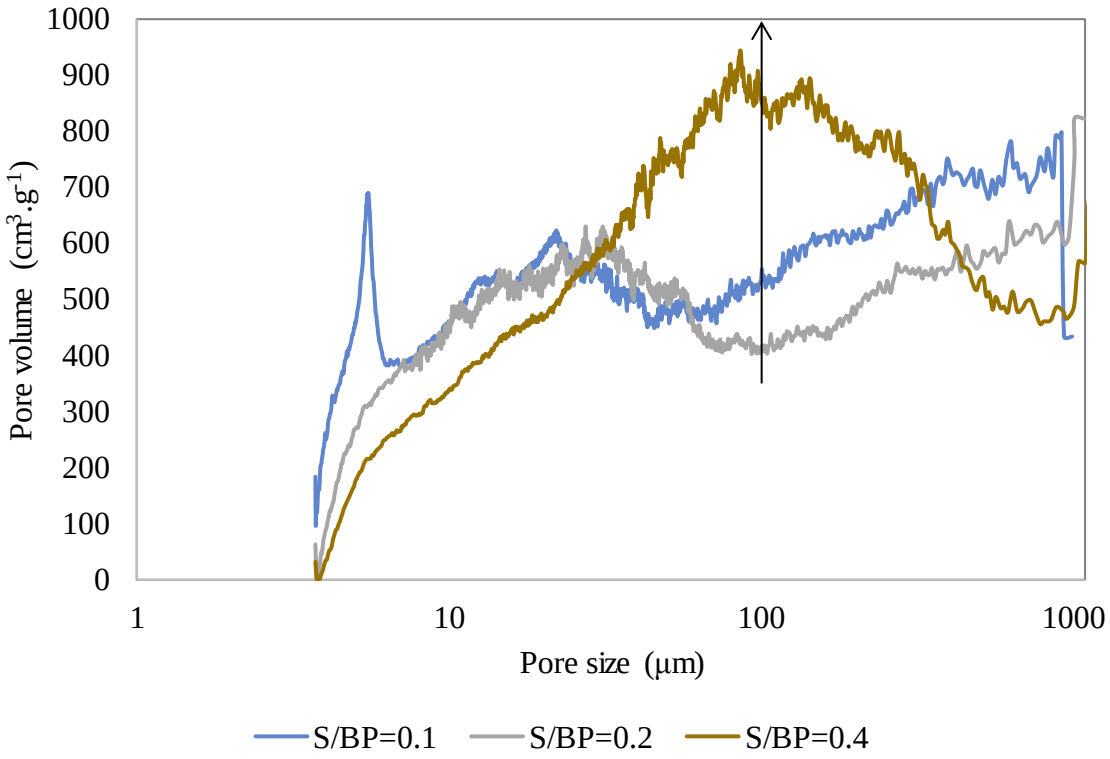

Figure 12: Pore distribution in the starch-beet composite

2.2.Sound absorption coefficient

Sound absorption coefficient of the bio-composite depends on the pore distribution, the connectivity between the various porous networks and the type of the binder [14,32].

In this present study, four formulations with different mass ratio S/BP were analyzed to investigate the influence of starch amount and humidity content. Figure 13 shows the results obtained using Kundt tube. For medium and high frequencies, the sound absorption coefficient tends to increase when the mass ratio S/BP increases from 0.1 to 0.4. It can be explained that the starch binder fills the pores and decreases the composite ability to dissipate the sound waves.

The highest sound absorption coefficient recorded for beet pulp-starch composite achieved about 0.72 at 4000 Hz with mass ratio S/BP equal 0.1. for the medium frequencies, the absorption of S-BP composite is 0.6, while the absorption of hemp-starch and cork composites is 0.4 and 0.28 respectively at the same frequency [12,14,32].

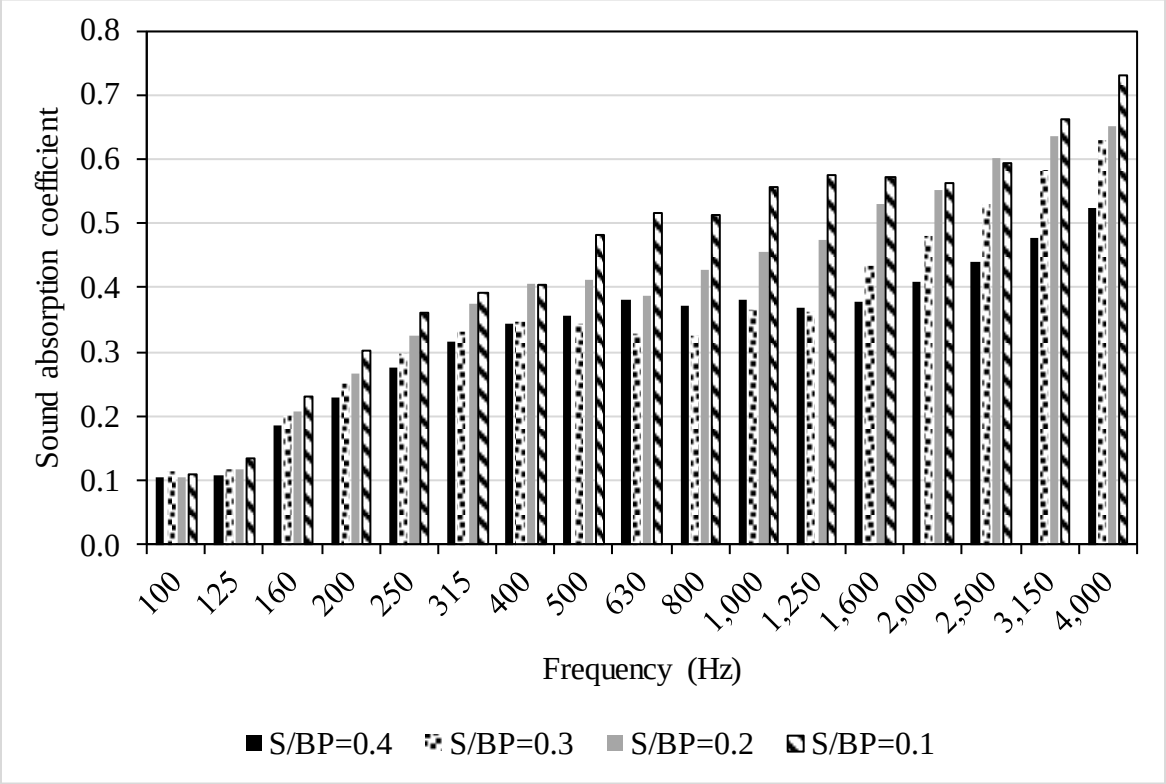

Figure 13: Sound absorption coefficient variation as function of frequencies.

The apparent histogram in Figure 14 represents the variation of the acoustic absorption coefficient α for a composite having a mass ratio S/BP = 0.3, as a function of different relative humidity of the climatic chamber (10% RH, 50% RH and 75% RH) in which the composite was stabilized and

at a constant temperature of 23 ° C. It is remarkable that the sound absorption coefficient increases slightly when the relative humidity increases from 10% to 75%. This can be explained by increasing relative humidity in the climatic chamber the moisture content in the composite increases, therefore the water molecules clog the micropores, resulting in a reduced porosity thus, the ability of the composite to absorb or dampen the incident sound signals with small wavelength (high frequencies). For medium frequencies, the composite subjected to 50% RH shows a better acoustic performance, which means ambient conditions the starch-beet composite works better than in other conditions. At low frequencies, the acoustic behavior of the composite is reversed, the sound absorption coefficient increases with relative humidity, it can be explained that at a high humidity (75% RH) the binder existing in the macro pores is plasticized and able to damper sound waves with long wavelength (low frequencies).

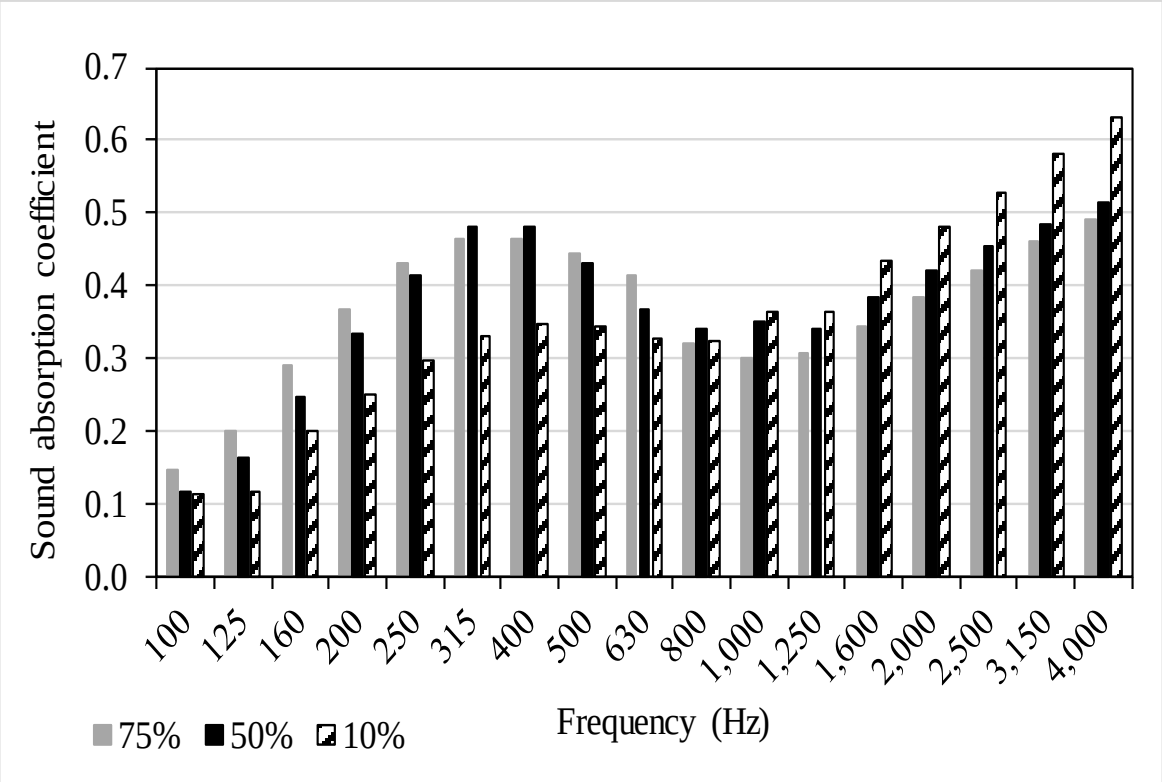

Figure 14: Sound absorption coefficient of beet-starch composite as a function of moisture content.

2.3.Thermal conductivity

The thermal effusivity and diffusivity is strongly related to the binder content (starch). Increasing the binder content in the composite promotes the thermal effusivity and decreases the thermal diffusivity. Thus, the starch content increases the composite ability to store heat.

Thermal conductivity of starch-beet pulp composite is comparable to hemp-starch composite (between 0.063 W. m-1. K-1 and 0.100 W. m-1. K-1) [2,7]. But it is greater than others composites such as hemp-clay and cork concrete [8,11]. Thus, leads to a better thermal inertia compared to hemp-starch composite [2,7,8].

Table 3 shows the thermal properties of starch-beet pulp composites for different mass ratio S/BP. The results show that the thermal conductivity λ increases linearly from 0.069 W. m-1. K-1 to 0.075 W. m-1. K-1 when the mass ratio S/BP increases from 0.1 to 0.4. the thermal conductivity can be expressed as function of the mass ratio S/BP according the equation (9). The increase of starch amount in S/BP composite decreases the composite porosity by filling the micropores, therefore the thermal conductivity increases.

The thermal diffusivity a is a physical quantity that characterizes the ability of a continuous material to transmit a temperature signal from one point to another of this material. It is calculated according to the equation (10) where ρ_{app} is the apparent density ($kg.m^{-3}$) and C_p is the heat capacity ($J.K^{-1}.kg^{-1}$).

The thermal effusivity ($J.K^{-1}.m^{-2}.s^{-1/2}$) b represents the ability of the composite to exchange thermal energy with its environment. The thermal effusivity is given by the equation (11)

$$\lambda = 0.0197 \times \frac{S}{BP} + 0.0673 \quad (9)$$

$$a = \frac{\lambda}{\rho_{app} \times C_p} \quad (10)$$

$$b = \sqrt{\lambda \times \rho_{app} \times C_p} \quad (11)$$

The thermal effusivity and diffusivity is strongly related to the binder content (starch). Increasing the binder content in the composite promotes the thermal effusivity and decreases the thermal diffusivity. Thus, the starch content increases the composite ability to store heat.

Thermal conductivity of starch-beet pulp composite is comparable to hemp-starch composite (between 0.063 W. m^{-1}. K^{-1} and 0.100 W. m^{-1}. K^{-1}) [2,7]. But it is greater than others composites such as hemp-clay and cork concrete [8,11]. Thus, leads to a better thermal inertia compared to hemp-starch composite [2,7,8].

Table 3: Thermal properties of starch-beet pulp composites at 23 °C.

Mass ratio (S/BP)	λ (W. m^{-1}. K^{-1})	a ($m^2.s^{-1}$)	b ($J.K^{-1}$. m^{-2}. $s^{-1/2}$)
0.1	0.069 ± 0.0006	1.76 ± 0.058E-07	165.5 ± 3.6
0.2	0.071 ± 0.0005	1.66 ± 0.0713E-07	175.2 ± 3.8
0.3	0.072 ± 0.0003	1.50 ± 0.052E-07	186.8 ± 3.5
0.4	0.075 ± 0.0002	1.47 ± 0.042E-07	197.5± 5.7

The solid thermal conductivities of the composites vary between 0.26 W. m^{-1}. K^{-1} and 0.30 W. m^{-1}. K^{-1}. That of beet pulp is 0.3151 W. m^{-1}. K^{-1} which is greater to that of the starch gel (λ_s=0.2314 W.m^{-1}. K^{-1}). Therefore, the increase of the composite thermal conductivity is due to the increase of the starch amount and the decrease of composite porosity by filling the macro pores.

The self-consistent scheme was applicated to estimate the beet pulp and solid thermal conductivities λ_s in agro-composites, with two phase model, from thermal conductivities measured by the Isomet method, absolute densities and total porosities measured by the cyclohexane method. Results are shown in Table4.

Table 4: Thermal conductivities of apparent agro-materials λ_{exp}, solid particles λ_s at 23 °C according to the self-consistent scheme.

Samples	λ_{exp} (W. m^{-1}. K^{-1})	n	λs
S/BP 0.1	0.069	0.7779	0.299
S/BP 0.2	0.071	0.7559	0.283
S/BP 0.3	0.072	0.7413	0.272
S/BP 0.4	0.075	0.7216	0.267
Beet pulp	0.062	0.8193	0.315
Starch gel	0.1396	0.3857	0.2411

2.4.Permeability

The water vapor permeability results are shown in the Table 5. The increase of binder amount tends to decrease the water vapor permeability of the starch-beet pulp composite. The sample with mass ratio S/BP = 0.1 contains macro-pores higher than the other. Therefore, the permeability of the composites depends mainly on the porosity [2]. Compared with hemp concrete the water vapor permeability of starch-beet pulp composites (8.90 x 10^{-12} kg. m^{-1}. s^{-1}. Pa^{-1}) is lower than that of hemp-starch composites (1.7-6.2 x 10^{-11} kg. m^{-1}. s^{-1}. Pa^{-1}) [4] and Typha-clay composites (2.83-6.15 x 10^{-11} kg. m^{-1}. s^{-1}. Pa^{-1}) [2]. This can be explained by the small size of the beet pulp (2-4 mm) which provides a composite more homogenous and less porous than the other.

Table 5: Permeability and resistance to water vapor of starch-beet pulp composites.

Mass ratio (S/BP)	δ x 10^{-12} (kg. m^{-1}. s^{-1}. Pa^{-1})	μ
0.1	8.90 ± 0.211	22.48 ± 0.54
0.2	7.77 ± 0.169	25.72 ± 0.55
0.3	7.35 ± 0.154	27.20 ± 0.58
0.4	6.86 ± 0.236	29.12 ± 1.01

2.5. Sorption isotherm

Figure 15 (a) shows the sorption isotherm curves of different samples of the four studied formulations. These curves describe the equilibrium between the medium relative humidity and the humidity content of the samples at 23 °C. According to the IUPA classification this is a typical behavior of cellulosic materials [41,42]. The samples show the same behavior independently of the mass ratio S/BP. This can be explained by the water adsorption which depends on two parameters: the porosity and the starch amount. The pores can store humidity by capillary condensation in the composite, known that the binder based on the starch is a hydrophilic material. Increasing the mass ratio S/BP means that the starch amount increases, and the porosity decreases. These parameters balance the water adsorption of the composites.

Figure 15 (b, c, d) shows the experimental values fitting according to GAB [37] , Merakeb [38] , and Van Genuchten [39] models. Among these models, the Van Genuchten seems to be the one that least close to the experimental values.

Table 6 shows the model parameters used to fit the sorption isotherm at 23 °C for the different formulations. For GAB and Merakeb models, E values are lower than 10 and the correlation coefficients for all models used are close to 1. Thus, GAB and Merakeb models are considered appropriate [43].

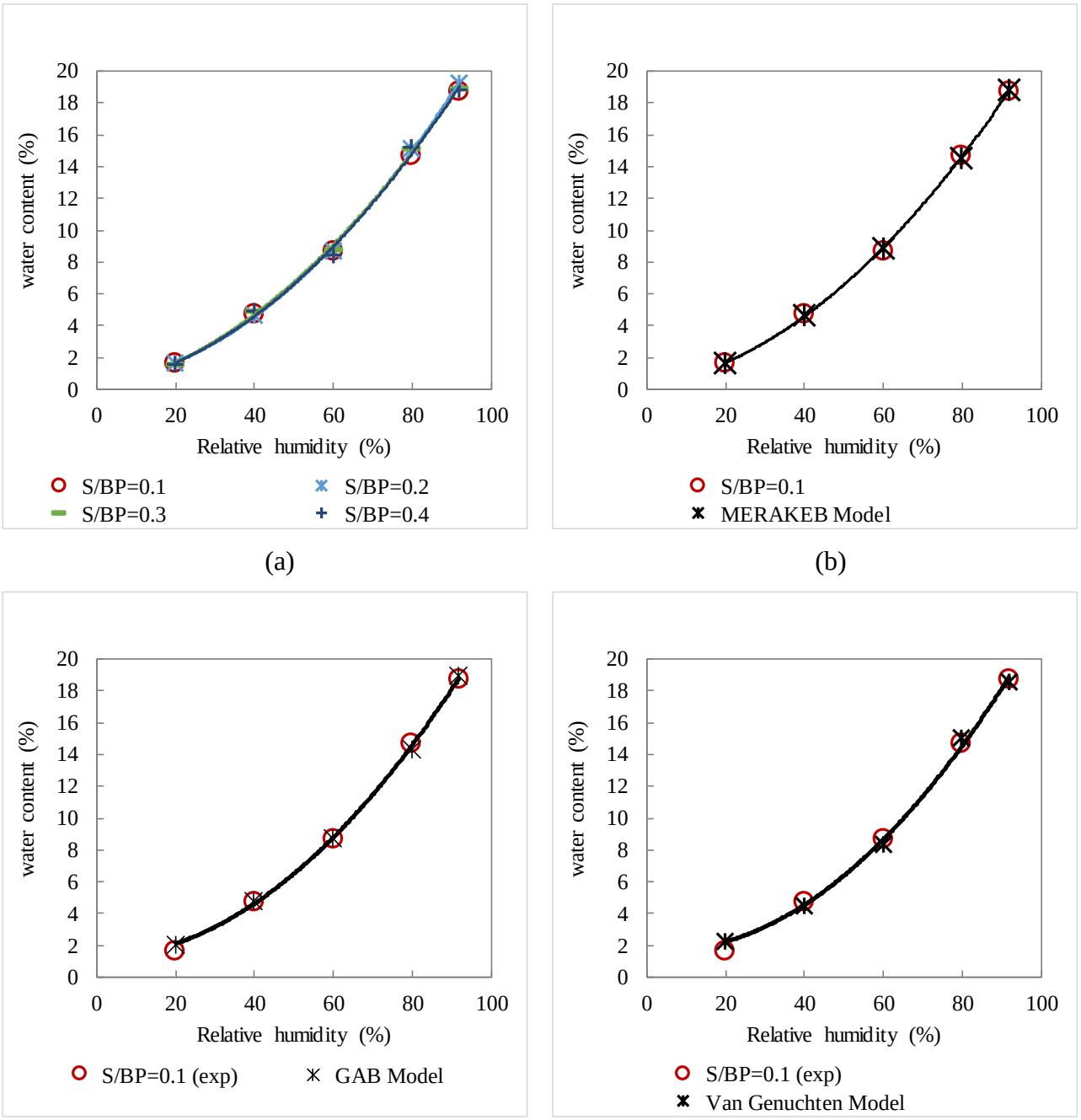

Figure 15: (a) Sorption isotherms of Starch-Beet pulp materials for the four formulations and the comparison of the experimental data with Merakeb (b) GAB (c) and Van Genuchten (d) models.

Table 6: Parameter values for the sorption isotherm models.

Models	Parameters	Samples S/BP= 0.1
Merakeb	a	1.5425
	b	0.2410
	u_s	0.2211
	E (%)	1.1689
	R^2	0.9998
	RMSE	0.1114
GAB	W_m	2.2848
	C_G	0.0938
	K	0.4024
	E (%)	5.5864
	R^2	0.9994
	RMSE	0.2484
Van Genuchten (VG)	U_s	0.1921
	η_T	2.2379
	α_T	0.0002
	E (%)	10.4050
	R^2	0.9982
	RMSE	0.3936

2.6. MBV

Figure 16 shows water content variation of beet pulp-starch composites during variations of relative humidity between 33 % and 75 % at 23 ˚C, where m_w the absorbed or released water mass and m_0 the sample initial mass. It can be seen the ability of the composite to absorb moisture at 75 %RH and to release moisture at 33 %RH. For the last three cycles, the mass variation of the samples appears to have stabilized.

The results presented in Table 7 clearly show that the composite can be classified an excellent regulator of the relative humidity of the environment (MBV> 2 g. m^{-2}. $\%RH^{-1}$) according to the

classification proposed by Rode [40]. The samples present MBV values between 2.6 and 2.8 g. $\%RH^{-1}.m^{-2}$, which are comparable with the MBV values of hemp-starch composites [7].

It can be observed that the variation in moisture buffering value as a function of the mass ratio S/BP is linear and can be presented by the Equation (12). Table 7 shows that increasing the mass of starch, tends to increase the MBV value, because of starch high moisture buffering. The samples with more starch, have the highest MBV value, around 2.80 g. $\%RH^{-1}.m^{-2}$.

Table 7: Moisture buffer values.

Sample S/BP	MBV (g. $\%RH^{-1}.m^{-2}$)	SD
0.1	2.62	0.060
0.2	2.68	0.065
0.3	2.72	0.080
0.4	2.80	0.090

This real value is to be compared to an ideal value (MBV_{ideal}) which neglects the resistance of the air layer to the surface of the material. The MBV_{ideal} is the limit value of MBV_{real} when the mass convection coefficient is infinite, and it is given by the relation in equation 12 [40]:

$$MBV_{ideal} = 0.00568 \times P_{sat} \times E_{ff} \times \sqrt{\tau} \quad (12)$$

$$E_{ff} = \sqrt{\frac{\delta \times \rho_0 \times \xi}{P_{sat}}} \quad (13)$$

where P_{sat} the saturation pressure (Pa), E_{ff} the hydric effusivity (kg. m^{-2}. Pa^{-1}. $s^{-1/2}$) calculated according the equation 13, δ the water vapor permeability ($kg.m^{-1}. s^{-1}.Pa^{-1}$), ρ_0 the apparent density ($kg.m^{-3}$), ξ the water capacity obtained by the derivative of the sorption curve (kg/kg) and τ the cycle period (24h = 86400 s). Table 8 shows the MBV_{ideal} of beet pulp -starch composite with relative humidity equal 75%. The ideal values increase with mass ratio S/BP as confirmed by experimental measurements. However, they are between 1.5 and 2 g. m^{-2}. $\%RH^{-1}$ which can be classified a good humidity regulator.

Table 8: Ideal moisture buffer values.

Mass ratio S/BP	ξ (kg/kg)	E_{ff} x 10^{-7} (kg. m^{-2}. Pa^{-1}. $s^{-1/2}$)	MBV_{ideal} (g. m^{-2}. $\%RH^{-1}$)
0.1	0.2380	5.23	1.82
0.2	0.2462	5.25	1.83
0.3	0.2412	5.29	1.86
0.4	0.2416	5.33	1.87

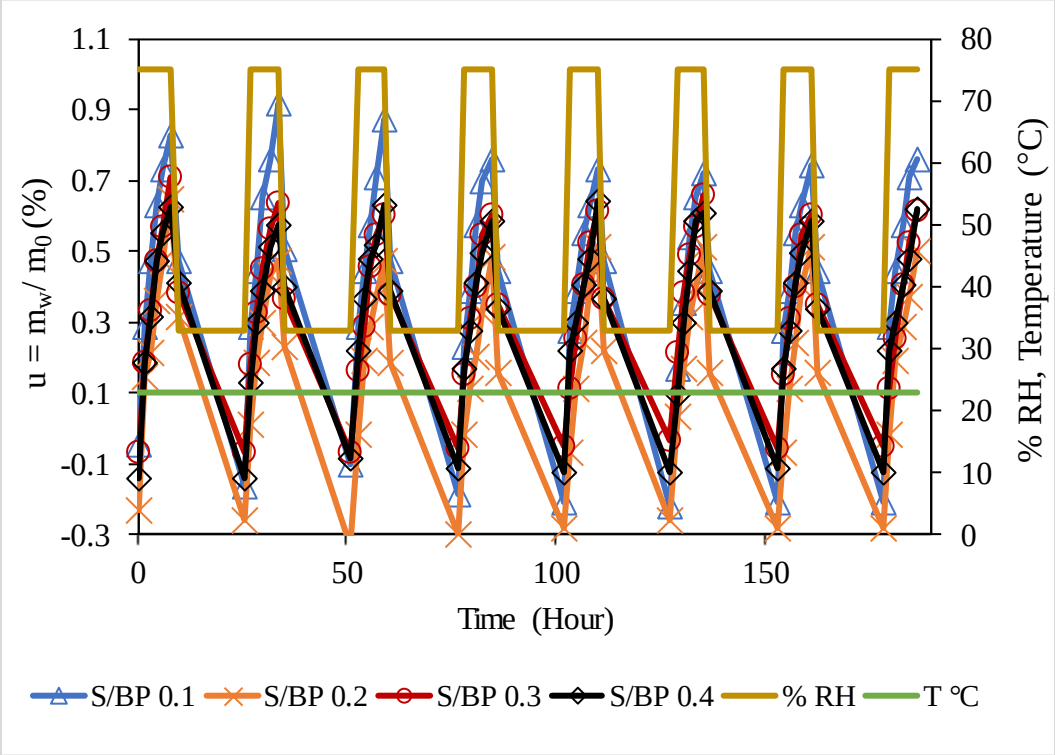

Figure 16: Moisture uptake and release for the BP-starch concrete during cyclic relative humidity variation in climatic chamber.

$$MBV = 0.62 \times \left(\frac{S}{BP}\right) + 2.55 \quad (14)$$

3. Conclusions

In this paper, the hygrothermal and acoustical properties of a Starch-Beet pulp composite were analyzed. Four formulations were studied with different mass ratio S/BP (0.1, 0.2, 0.3 and 0.4) to

investigate the influence of the starch amount and the porosity on composite characterizations. Two classes of pores can be determined in the starch-beet composites (macro pores and meso pores). The sound absorption coefficient of the composite depends on the humidity amount and the porosity. The better acoustical performance was obtained under ambient conditions (50 %RH and 23 °C) and with lower starch amount (S/BP = 0.1).

The measure of the thermal conductivity and the thermal inertia (thermal diffusivity and effusivity) shows that the Starch-Beet pulp composite provides a good thermal insulator. The increase of starch amount tends to increase the thermal conductivity of the composites.

The results show that the water vapor permeability depends on the porosity and he MBV increases linearly from 2.6 g/m^2. K to 2.8 g/m^2. K when the mass ratio S/BP increases from 0.1 to 0.4. The Rode classification shows that the starch-Beet pulp composite is an excellent moisture regulator. However, the sorption isotherm is independent of the mass ratio S/BP.

References

[1] Cerolini S, D'Orazio M, Di Perna C, Stazi A. Moisture buffering capacity of highly absorbing materials. Energy Build 2009;41:164–8. doi:10.1016/j.enbuild.2008.08.006.

[2] Niang I, Maalouf C, Moussa T, Bliard C, Samin E, Thomachot-Schneider C, et al. Hygrothermal performance of various Typha–clay composite. J Build Phys 2018. doi:10.1177/1744259118759677.

[3] EU Commision. Trends to 2050. 2013. doi:10.2833/17897.

[4] Collet F, Chamoin J, Pretot S, Lanos C. Comparison of the hygric behaviour of three hemp concretes. Energy Build 2013;62:294–303. doi:10.1016/j.enbuild.2013.03.010.

[5] Maalouf C, Ingrao C, Scrucca F, Moussa T, Bourdot A, Tricase C, et al. An energy and carbon footprint assessment upon the usage of hemp- lime concrete and recycled-PET façades for of fi ce facilities in France and Italy. J Clean Prod 2018;170:1640–53. doi:10.1016/j.jclepro.2016.10.111.

[6] Moussa T, Maalouf C, Ingrao C, Scrucca F, Asdrubali F. Bio-based and recycled-waste materials in buildings : A study of energy performance of hemp- lime concrete and recycled-PET façades for office facilities in France and Italy 2018;4731.

doi:10.1080/23744731.2018.1438664.

[7] Bourdot A, Moussa T, Gacoin A, Maalouf C, Vazquez P, Thomachot-Schneider C, et al. Characterization of a hemp-based agro-material: Influence of starch ratio and hemp shive size on physical, mechanical, and hygrothermal properties. Energy Build 2017;153:501–12. doi:10.1016/j.enbuild.2017.08.022.

[8] Mazhoud B, Collet F, Pretot S, Lanos C. Development and hygric and thermal characterization of hemp-clay composite. Eur J Environ Civ Eng 2017;8189:1–11. doi:10.1080/19648189.2017.1327894.

[9] Moussa T, Maalouf C, Lachi M, Umurigirwa S, Mai TH, Henry J-F. Development and performance evaluation of a hemp–starch composite. J Build Phys 2016;40:278–95. doi:10.1177/1744259116637860.

[10] B.S. UMURIGIRWA-VASSEUR. Elaboration et caractérisation d ' un agromatériau chanvre-amidon pour le Bâtiment. PhD Thesis REIMS University, 9 december 2014., 2014.

[11] Boussetoua H, Maalouf C, Lachi M, Belhamri A, Moussa T. Mechanical and hygrothermal characteri **s** ation of cork concrete composite: experimental and modelling study. Eur J Environ Civ Eng 2017;8189:1–16. doi:10.1080/19648189.2017.1397551.

[12] Gourlay E, Glé P, Marceau S, Foy C, Moscardelli S. Virtual Special Issue Bio Based Building Materials Effect of water content on the acoustical and thermal properties of hemp concretes 2017;139:513–23. doi:10.1016/j.conbuildmat.2016.11.018.

[13] Rahim M, Douzane O, Tran Le AD, Langlet T. Effect of moisture and temperature on thermal properties of three bio-based materials. Constr Build Mater 2016;111:119–27. doi:10.1016/j.conbuildmat.2016.02.061.

[14] Glé P, Gourdon E, Arnaud L. Acoustical properties of materials made of vegetable particles with several scales of porosity. Appl Acoust 2011;72:249–59. doi:10.1016/j.apacoust.2010.11.003.

[15] Arnaud L, Gourlay E. Experimental study of parameters influencing mechanical properties of hemp concretes. Constr Build Mater 2012;28:50–6.

doi:10.1016/j.conbuildmat.2011.07.052.

[16] Le AT, Gacoin A, Li A, Mai TH, Rebay M, Delmas Y. Experimental investigation on the mechanical performance of starch-hemp composite materials. Constr Build Mater 2014;61:106–13. doi:10.1016/j.conbuildmat.2014.01.084.

[17] Roge, B. M. L'Extraction Du Sucre. Reims: 2005.

[18] Nasielski S. Le bon usage de la pulpe surpressée. vol. 132. Tienen (Tirlemont), Belgique: 2009. doi:10.3917/aatc.132.0001.

[19] Sun R, Hughes S. Extraction and physico-chemical characterization of pectins from sugar beet pulp. Polym J 1998;30:671–7. doi:10.1295/polymj.30.671.

[20] PHATAK L, CHANG KC, BROWN G. Isolation and Characterization of Pectin in Sugar-Beet Pulp. J Food Sci 1988;53:830–3. doi:10.1111/j.1365-2621.1988.tb08964.x.

[21] Chen HM, Fu X, Luo ZG. Properties and extraction of pectin-enriched materials from sugar beet pulp by ultrasonic-assisted treatment combined with subcritical water. Food Chem 2015;168:302–10. doi:10.1016/j.foodchem.2014.07.078.

[22] Dronnet VM, Renard CMGC, Axelos MAV, Thibault J-F. Binding of divalent metal cations by sugar-beet pulp. Carbohydr Polym 1997;34:73–82. doi:10.1016/S0144-8617(97)00055-6.

[23] Monreal P, Mboumba-Mamboundou LB, Dheilly RM, Quéneudec M. Effects of aggregate coating on the hygral properties of lignocellulosic composites. Cem Concr Compos 2011;33:301–8. doi:10.1016/j.cemconcomp.2010.10.017.

[24] Boursier B. Amidons natifs et amidons modifiés alimentaires. Tech L'ingénieur Additifs Adjuv Aliment 2005;33:27.

[25] Zaidul ISM, Absar N, Kim S, Suzuki T. DSC study of mixtures of wheat flour and potato , sweet potato , cassava , and yam starches 2008;86:68–73. doi:10.1016/j.jfoodeng.2007.09.011.

[26] Zaidul ISM. RVA analysis of mixtures of wheat flour and potato , sweet potato , yam , and cassava starches 2007;69:784–91. doi:10.1016/j.carbpol.2007.02.021.

[27] Jobling S. Improving starch for food and industrial applications 2004:210–8. doi:10.1016/j.pbi.2003.12.001.

[28] J.O.B. Carioca, H.L. Arora, P.V.P. Selvam, F.C.A. Tavares, J.F. Kennedy CJK. Industrial Utilisation of Starch and its Derived Products in Brazil. Stärke 48 1996;48:322–6.

[29] R.L. Whistler JRD. 1. Physical Properties. Starch, Kirk-Othmer Encycl Chem Technol, JohnWiley Sons, Inc, Hoboken, NJ, USA, 2000 n.d.

[30] Wertz J-L. L'amidon et le PLA : deux biopolymères sur le marché. Wallone, Belgium: 2011.

[31] Belhamri R. Extraction des macromolécules pariétales des eaux de presse de betteraves sucrières : Etude de leur composition, de leurs propriétés physico-chimiques et de leur effet sur le process sucrier. Phd Thesis Reims University, 25 february 2005, 2005.

[32] Belakroum R, Gherfi A, Bouchema K, Gharbi A, Kerboua Y, Kadja M, et al. Hygric buffer and acoustic absorption of new building insulation materials based on date palm fibers. J Build Eng 2017;12:132–9. doi:10.1016/j.jobe.2017.05.011.

[33] Samri D. Analyse physique et caractérisation hygrothermique des matériaux de construction: approche expérimentale et modélisation numérique. 2009.

[34] Haba B, Agoudjil B, Boudenne A, Benzarti K. Hygric properties and thermal conductivity of a new insulation material for building based on date palm concrete. Constr Build Mater 2017;154:963–71. doi:10.1016/j.conbuildmat.2017.08.025.

[35] Collet F, Prétot S. THERMAL CONDUCTIVITY OF HEMP CONCRETES : VARIATION WITH FORMULATION , DENSITY AND WATER CONTENT Florence Collet , Sylvie Prétot To cite this version : HAL Id : hal-01003739 2014.

[36] Shivhare US, Arora S, Ahmed J, Raghavan GS V. Moisture adsorption isotherms for mushroom 2004;37:133–7. doi:10.1016/S0023-6438(03)00135-X.

[37] Anderson B. Modifications of the Brunauer, Emmett and Teller Equation1 1940;1:686–91.

[38] Seddik Merakeb, Frédéric Dubois CP. Modeling of the sorption hysteresis for wood ´.

Wood Sci Technol 2009;575–589:575–89. doi:10.1007/s00226-009-0249-2.

[39] Genuchten VAN. A Closed-form Equation for Predicting the Hydraulic Conductivity of Unsaturated Soils 1 n.d.;8:892–8.

[40] Rode C, Peuhkuri R, Mortensen L., Hansen K., Time B, Gustavsen A, et al. Moisture Buffering of Building Materials Department of Civil Engineering Technical University of Denmark. 2005.

[41] Kenneth S. W. Sing, Douglas H. Everett, R. A. W. Haul, L. Moscou, Robert A. Pierotti, Jean Requerol and TS. Manual of Symbols and Terminology for Physicochemical Quantities and Units [3–5]. Pure Appl Chem 1985;57:603–19.

[42] Célino A, Fréour S, Jacquemin F, Casari P. The hygroscopic behavior of plant fibers : a review 2014;1:1–12. doi:10.3389/fchem.2013.00043.

[43] Ayranci E, Duman O. Moisture sorption isotherms of cowpea (Vigna unguiculata L . Walp) and its protein isolate at 10 , 20 and 30 ° C 2005;70:83–91. doi:10.1016/j.jfoodeng.2004.08.044.